Learning the Visualness of Text Using Large Vision-Language Models

Gaurav Verma[†], Ryan A. Rossi[‡], Christopher Tensmeyer[‡], Jiuxiang Gu[‡], Ani Nenkova[‡]

[†]Georgia Institute of Technology, [‡]Adobe Research
gverma@gatech.edu, {ryrossi,tensmeye,jigu,nenkova}@adobe.com

Abstract

Visual text evokes an image in a person's mind, while non-visual text fails to do so. A method to automatically detect visualness in text will unlock the ability to augment text with relevant images, as neural text-to-image generation and retrieval models operate on the implicit assumption that the input text is visual in nature. We curate a dataset of 3,620 English sentences and their visualness scores provided by multiple human annotators. Additionally, we use documents that contain text and visual assets to create a distantly supervised corpus of document text and associated images. We also propose a fine-tuning strategy that adapts large vision-language models like CLIP that assume a one-to-one correspondence between text and image to the task of scoring text visualness from text input alone. Our strategy involves modifying the model's contrastive learning objective to map text identified as non-visual to a common `NULL` image while matching visual text to their corresponding images in the document. We evaluate the proposed approach on its ability to *(i)* classify visual and non-visual text accurately, and *(ii)* attend over words that are identified as visual in psycholinguistic studies. Empirical evaluation indicates that our approach performs better than several heuristics and baseline models for the proposed task. Furthermore, to highlight the importance of modeling the visualness of text, we conduct qualitative analyses of text-to-image generation systems like DALL-E.

1 Introduction

People typically communicate knowledge and information textually, but most prefer visually rich content. Text-to-image generation/retrieval models could augment text with appropriate associated images, aiding the creation of appealing and easy-to-understand documents. Recent models like DALL-E (Ramesh et al. 2021a, 2022) and Stable Diffusion (Rombach et al. 2022) work phenomenally well for input text that is carefully constructed to elicit images. However, they cannot handle long text that may or may not evoke a visual image. We introduce the task of quantifying *sentence visualness*—a term we use interchangeably with *imageability*—as a necessary first step toward connecting textual documents with visual assets. Consider the following two examples: "*The flowerheads of Haemanthus coccineus ..., with scarlet spathe valves on them like bright shaving brushes, make it a striking plant*" ($\mathcal{V}$) and "*A copyright notice is a notice of statutorily prescribed form that informs users of the underlying claim to copyright ownership in a published work*" ($\bar{\mathcal{V}}$). While $\mathcal{V}$ evokes an image in the reader's mind, $\bar{\mathcal{V}}$ will be considered non-visual by most.

Vision-language models like ViLBERT (Lu et al. 2019), CLIP (Radford et al. 2021), and UNITER (Chen et al. 2020) have achieved remarkable performance on tasks like Visual Question Answering (VQA) (Antol et al. 2015), cross-modal retrieval (Wang et al. 2016), and Visual Commonsense Reasoning (VCR), but it is not clear how well these models can distinguish visual text from non-visual text. Text-to-image generation models like DALL-E and Imagen (Saharia et al. 2022) would benefit from inferring text visualness *before* they can generate images to embellish textual documents. In Figure 1a, we demonstrate the need with some examples: text identified to have low visualness leads to irrelevant generations from DALL-E, while text identified to have high visualness leads to the generation of relevant images.

Prior approaches quantifying the visualness of text operate on a word or phrase level (Deschacht and Moens 2007; Jeong, Wang, and Lee 2012) and leverage lexicons that contain human-assigned world-level imageability scores (Louis and Nenkova 2013). However, such techniques are limited in coverage and may not handle sentence-level visualness.

We curate a corpus of 3,260 sentences in English paired with their human ratings for visualness, as well as a noisy-but-large corpus of 48,077 automatic alignments between text and visual assets in documents, including a `NULL` non-visual image. The textual part of the resulting alignment pairs can be used as examples of visual and non-visual sentences. We propose a fine-tuning strategy for vision-language models like CLIP that allows classification inferences over text-only inputs. Our proposed objective also ensures that the learned embeddings remain usable for downstream tasks like text-to-image retrieval. We compare the performance of our proposed approach against several heuristic and model-based baselines. Our extensive evaluation suggests that our fine-tuning strategy leads to the most accurate visual and non-visual text classifier. Finally, we conduct several analyses to glean insights into the model's learned attention mechanism, text-to-image retrieval abilities, and downstream text-to-image generation capabilities.

Accepted non-archival work at Creative AI Across Modalities Workshop @ AAAI 2023.

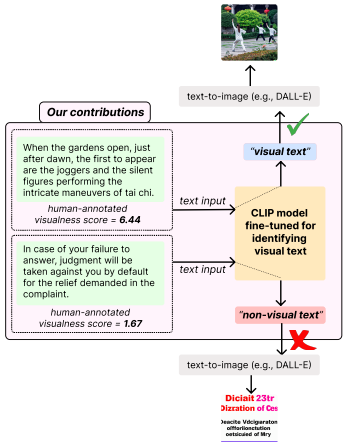

(a) Sentence visualness task

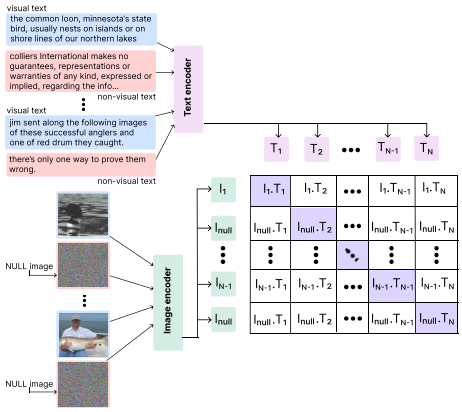

(b) Approach for sentence visualness prediction

Figure 1: **(a)**: The visual text identification task, along with a motivating downstream application. **(b)**: Our approach to predicting sentence visualness, with a fine-tuning strategy where visual text is matched with its corresponding image while non-visual text is matched with a fixed NULL image.

2 Related Work

There are two research themes related to our work: *(i)* large vision-language models and their adaptations to downstream multimodal tasks, and *(ii)* understanding and quantifying visualness of words.

Fine-tuning Vision-Language Models for Downstream Tasks: Vision-Language models aim to process and relate information across the visual and language modalities (Baltrušaitis, Ahuja, and Morency 2018; Yuan et al. 2021; Radford et al. 2021; Lu et al. 2019; Tan and Bansal 2019). Large models like CLIP (Radford et al. 2021), UNITER (Chen et al. 2020), and ALIGN (Jia et al. 2021) have demonstrated remarkable performance on downstream tasks via transfer learning or fine-tuning. However, such downstream tasks assume *both* text and image as input to determine similarity or generate/retrieve the other modality for *every* instance of the corresponding modality; for instance, visual question answering (Antol et al. 2015), caption generation (Xu et al. 2015), and cross-modal retrieval (Wang et al. 2016). Fine-tuning large vision-language models on such downstream tasks involves adding components to the encoders' architecture and training additional parameters on the task-specific dataset; the additional components could be fusion layers with cross-attention for multimodal classification (Mittal et al. 2022), or a Transformer-based generation module for caption generation (Sarto et al. 2022). Transferability and reusability of models and their learned representations to downstream tasks and other domains are also a desirable properties (Yosinski et al. 2014; Long et al. 2015), especially in light of catastrophic forgetting (Goodfellow et al. 2013).

Our work differs from existing work in that the input is only text, requiring us to adapt large vision-language models to not rely on both modalities during inference. We propose a fine-tuning strategy that does not involve additional architectural components (and parameters) on top of a pre-trained CLIP architecture and yet effectively adapts CLIP for learning text visualness. Our task can be considered a precursor to tasks like text-to-image retrieval and generation, where images are only retrieved or generated for visual text. Further, we aim to preserve the reusability of text embeddings learned for the visualness categorization task for downstream tasks like text-to-image retrieval.

Visualness of Words: The visualness of text has been studied in multiple prior works but at a word or phrase level. Coltheart (1981) curated the MRC Psycholinguistic Database comprising human ratings for word-level imageability. Since the lexicon only contains scores for 3769 words, the limited coverage of these visualness ratings has been a major limitation. Louis and Nenkova (2013) address this challenge by assuming that visual tags for images tend to co-occur with other visual terms. They use topic modeling over image tags and consider tags co-occurring in the same topic as visual words in the MRC lexicon to be visual. Beyond word-level visualness, some studies have focused on phrase-level visualness. For instance, Jeong, Wang, and Lee (2012) quantify the visualness of a concept like 'round table' and 'red tomato' by measuring the "visual purity" and entropy of the clusters of images retrieved for that concept. In the same vein, Deschacht and Moens (2007) quantify the visualness of an entity mention on Wikipedia by computing its synsets similarity with a collection of 25 synsets that are manually labeled for their visualness (In WordNet (Miller 1995), synset is a collection of words that have a close meaning and that represent an underlying concept).

Our work focuses on learning sentence-level visualness instead of word or phrase-level visualness. While it is possible to aggregate word-level and phrase-level visualness scores to obtain sentence-level scores, it is unclear how accurate and generalizable these techniques are. We design multiple baselines that use word-level visualness scores to quantify sentence-level visualness and contrast the performance of such approaches with our proposed approach.

3 Text Imageability Dataset (TImeD)

Our proposed fine-tuning approach follows multi-stage training of a large vision-language model CLIP (Radford et al. 2021). In the first stage, we conduct large-scale fine-tuning, followed by fine-tuning on a relatively smaller annotated corpus in the second stage. We first discuss the curation of a large-scale corpus that comprises automatically-assigned and distant labels and then describe the curation of the human-labeled corpus of visual & non-visual sentences.

3.1 Dataset for fine-tuning with automatic labels

As we will discuss in the following section, the formulation of the training objective requires positive examples comprising visual text and paired images as well as negative examples that comprise non-visual text. To create a corpus like this, we: *(i)* leverage image-text co-occurrences in documents to develop a self-supervised approach, and *(ii)* use image-text similarity scores obtained using CLIP as priors to construct a large training corpus. We start with 450,000 publicly available PDFs referenced in the Common Crawl corpus and identify pages within those PDFs that include images.[1] We use a document object detection tool like Fitz[2] to extract paragraphs and images from the document pages.

We do sentence segmentation for the identified paragraphs using NLTK Tokenizer (Bird 2006). To map the images in the page to sentences, we compute CLIP similarity scores between each image-sentence pair in a given page. Based on the distribution of image-sentence similarity scores across all the pages in our corpus, we set two thresholds, T_{pos} and T_{neg}. A sentence in a page is considered a positive example (visual text) if its similarity with *any* of the images in the page is greater than T_{pos}. Similarly, chosen negative examples have similarity values less than T_{neg} with *all* images within the same page. Sentences with an image similarity value greater than T_{pos} are associated with the most similar image in the same page, while the negative examples are associated with a common `NULL` image. The thresholds T_{pos} and T_{neg} are chosen conservatively to only include top or bottom k % sentences from the entire corpus, respectively. This limits the noise in our training corpus for adapting the CLIP model for scoring text imageability. In our experiments, we set T_{pos} to be 0.35 to consider top 1% sentences as visual and T_{neg} to be 0.18 to consider bottom 5% sentences as non-visual. Our automatically-labeled corpus comprises 15,359 visual sentences, the corresponding images, and 32,718 non-visual sentences.

3.2 Human-annotated dataset

For the human-annotated visual and non-visual examples, we start with another 200,000 PDFs distinct from those used for the automated assignment of labels. To focus on natural images rather than infographics and academic figures, we filtered these documents to only include brochures, flyers, and magazines. For the resulting 35,432 documents, we adopted the same policy as that for curating the automatically-labeled dataset (selecting top 1% and bottom 5% sentences based on similarity values). We then recruited annotators to rate the visualness of the resulting 3,620 sentences after manually anonymizing any Personal Identifiable Information (PII) instances.

We recruited annotators on Amazon Mechanical Turk (AMT). We randomly ordered the 3,620 examples and, for each example, we asked nine annotators to provide a response on a 7-point Likert scale for the following question: "*Do you agree that the sentence below evokes an image or picture in your mind?*" A response of 1 indicated strong disagreement, while 7 indicated strong agreement. We also inserted some attention-check examples (5%; $n = 181$) to ensure the annotators read the text carefully before responding. These checks explicitly asked the annotators to mark a randomly-chosen score on the Likert scale regardless of the actual content. We discarded the annotations from annotators who did not correctly respond to all the attention-check examples and re-collected more responses iteratively. Appendix 8.3 provides details about the demographic filters for the recruited annotator and the annotation interface.

If a majority of annotations (i.e., at least 5 out of 9) were 1, 2, or 3, we considered the example to be `non-visual` ($n = 2108$). Similarly, `visual` examples had a majority of 5, 6, or 7 responses ($n = 1132$). We considered examples that did not have a clear majority or majority of responses of 4 (i.e., 'Neutral' on the Likert scale) as `ambiguous` and `neutral`, respectively. Table 1 shows illustrative examples of `visual`, `non-visual`, and `ambiguous` text from our human-annotated corpus.

For 27.1% of the examples only at most 1 of the 9 annotators disagreed with the labels decided based on the process described above. Only 10.5% of the sentences were assigned a neutral or ambiguous class. Inter-annotator agreement measured by Krippendorff's α was 0.446. Krippendorf's α quantifies the degree of agreement *beyond* that by chance (i.e., observed disagreement over expected disagreement). Since the expected disagreement is strongly influenced by the ratio of values in the reliability matrix, the value is inherently small in our case as the annotator responses are skewed towards labels like 'Somewhat agree,' 'Disagree,' and 'Completely disagree' than the others. This inter-annotator agreement value is in a similar range to what is observed for other language-related tasks that involve assessment of text by *experts* on dimensions like coherence, likability, relevance, and even grammar (Karpinska, Akoury, and Iyyer 2021). For brevity, we refer to the curated dataset as TIMED, short for **T**ext **Im**ag**e**ability **D**ataset.

4 TIP-CLIP for Scoring Text Visualness

Background: The CLIP model (Radford et al. 2021) jointly trains image and text encoders to predict the correct pairing between images and textual descriptions. In a batch size of N images and N texts (N^2 possible image-text pairings), the objective function ensures that the cosine similarity between the embeddings of correct image-text pairs is maximized while the cosine similarity between the $(N^2 - N)$ incorrect image-text pairs is minimized. The encoders are trained over a large multimodal dataset comprising about 400 million image-text pairs.

Updated training objective: When predicting text visualness, the goal is to assign a higher score to text that is visual (evokes a concrete image for the person reading it) and a lower score for non-visual text (text that does not evoke an image). In line with the original training objective, we further train the CLIP model to match text that is identified as

[1] We choose to work with PDF documents rather than webpages because *(i)* PDFs have natural demarcations in the form of pages (whereas webpages often contain long-running text with complex image-text interactions), and *(ii)* images within a page are likely to be related to selected text fragments within the same page.

[2] https://github.com/pymupdf/PyMuPDF

Category	Example text	μ / σ
Visual	· now the snow has melted and the grass not only looks dreary, but it is soggy.	$\mu = 6.88$
	· The operation left a six-inch zipper scar on his chest.	$\mu = 6.55$
	· When the gardens open, just after dawn, the first to appear are the joggers and the silent figures performing the intricate maneuvers of tai chi.	$\mu = 6.44$
	· He removed the box, placed it next to the garbage can, and put his garbage inside the can.	$\mu = 5.88$
	· But, after running only the first 500 meters, he realized that the injury that seemed so insignificant would not only prevent him from winning the race, but also from finishing it.	$\mu = 5.00$
Non-visual	· There's only one way to prove them wrong.	$\mu = 1.22$
	· For more information or to schedule an outreach, please call (999) 123-4567 or email email@website.com.	$\mu = 1.55$
	· In case of your failure to answer, judgment will be taken against you by default for the relief demanded in the complaint.	$\mu = 1.67$
	· A 25% quorum of member votes in each district is needed to conduct district delegate elections in October.	$\mu = 1.77$
	· Colliers International makes no guarantees, representations or warranties of any kind, expressed or implied, regarding the information including, but not limited to, warranties of content, accuracy and reliability.	$\mu = 2.00$
Ambiguous	· J. Roman discusses his book Ohio State Football: The Forgotten Dawn which draws on extensive archival research to tell the untold story of the early days of football at Ohio as flagship public university.	$\sigma = 2.34$
	· Remember to be sure to set your clocks back 1 hour before you go to bed on Saturday, November 3rd.	$\sigma = 2.23$
	· That is the most important thing in my life today: Jesus.	$\sigma = 2.20$
	· Children & parents will get to hear author George McClements read his book Ridin' Dinos with Buck Bronco.	$\sigma = 2.14$
	· Financial Peace University is a nine-lesson class taught by financial expert Dave Ramsey through entertaining videos with an in-depth workbook, that will teach you how to take control of your money.	$\sigma = 2.16$

Table 1: Qualitative examples of visual and non-visual text from the human-annotated subset of the **T**ext **Im**ag**e**ability **D**ataset (based on the average of annotator ratings), and text with high ambiguity (based on the standard deviation of annotator ratings).

`visual` with the corresponding image. We adapt the CLIP training to match text that is identified as `non-visual` with a single `NULL` image (see Fig. 1b). Matching visual text with the corresponding image while non-visual text to a `NULL` image not only encourages the model to distinguish between visual and non-visual text, but also allows it to anchor non-visual text in the common `NULL` image that can be used during inference without having access to a potentially paired image. Formally, the adapted training objective is given as,

$$\mathcal{L} = -\frac{1}{2N}\sum_{j=1}^{N} log\left(\frac{exp(\langle I_j^e, T_j^e\rangle/\tau)}{\sum_{k=1}^{N} exp(\langle I_j^e, T_k^e\rangle/\tau)}\right) - \frac{1}{2N}\sum_{k=1}^{N} log\left(\frac{exp(\langle I_k^e, T_k^e\rangle/\tau)}{\sum_{j=1}^{N} exp(\langle I_j^e, T_k^e\rangle/\tau)}\right) \tag{1}$$

$$\text{such that, } I_m^e = \begin{cases} I_{null}^e, & \text{if } m \in \bar{\mathcal{V}} \text{ (i.e., non-visual)} \\ I_m^e, & \text{if } m \in \mathcal{V} \text{ (i.e., visual).} \end{cases} \tag{2}$$

Here, N denotes the number of examples in a batch, I_m^e and T_m^e denote the embeddings of the m-th pair of image and text that are normalized to have unit ℓ_2-norm, respectively, such that $m \in \{1, \ldots, N\}$. $\langle ... \rangle$ represents the inner product, and τ is the trainable temperature parameter. $\bar{\mathcal{V}}$ and $\mathcal{V}$ are the set of examples in the current batch that belong to non-visual and visual categories, respectively. Finally, I_{null}^e denotes the embedding of the `NULL` image. During inference, we compute the cosine similarity between the representation of a given text with the representation of the `NULL` image; non-visual texts will have a high similarity with the NULL image. Conversely, the visualness score $\mathcal{S}$ of any text with embedding T^e can be obtained using

$$\mathcal{S} = 1 - \langle I_{\texttt{NULL}}^e, T^e \rangle. \tag{3}$$

For the `NULL` image, we create an RGB image of size $(224, 224, 3)$ in which each pixel value is chosen randomly (see Figure 1b). However, experiments with different types of `NULL` images indicate that the choice of null image does not affect the model's performance; see Appendix 8.1.

An alternative formulation for adapting the CLIP training objective could have been to match visual text with a single image while matching non-visual text with a single `NULL` image. However, this formulation of the training objective is similar to binary classification and does not enforce a contrastive objective for the positive examples. Matching visual text with its corresponding image instead of a common image for all visual text affords text embeddings that can be used for downstream tasks like text-to-image retrieval; we provide empirical evidence for worse text-to-image retrieval performance with the alternative formulation in Results.

5 Training details and Baselines

Train, test, & validation splits: Recall that our fine-tuning approach requires paired images for visual sentences only during training time and not during inference time; the model needs only text as input during inference. Of the 1132 visual sentences in the human-annotated set of TIMED, we assign 515 examples that had an automatically determined corresponding image to the training set, and the remaining were randomly assigned to the test set ($n = 517$) and validation set ($n = 100$). The 2108 non-visual sentences were randomly split into the training ($n = 980$), test ($n = 928$), and validation set (200). All three sets maintain `positive:negative` class ratio of ~ 0.5.

For the first stage of training, we fine-tune the CLIP model (ViT/B-32) on the proposed objective (see Eq. 2) using the 48,077 examples with automatic labels. This training is done on Tesla T4 GPUs, for 5 epochs, with a batch size of 32, and a learning rate initialized at 5×10^{-5} and optimized using Adam optimizer (Kingma and Ba 2014). Following this, for the second stage, we further fine-tune the same model for 2 epochs using the same objective and hyper-parameters, but this time using the train set of human-annotated TIMED.[3] The hyper-parameters are selected by performing a grid search while observing performance on the validation set of TIMED. Based on the performance on the validation set of TIMED, we set the threshold of $\mathcal{S}$ (Eq. 3) to be 0.79 to categorize text as `visual` or `non-visual`. We refer to the model trained using our fine-tuning strategy as TIP-CLIP, short for **T**ext **I**mageability **P**redictor CLIP, and report performance on the test set of TIMED.

[3]The CLIP model has a maximum context length of 77 tokens (about 50 words). Fewer than 1% of the training examples across both stages of the training are truncated to fit this context length.

5.1 Baselines

We investigate the performance of TIP-CLIP against several heuristics and baseline models.

Random: The random baseline generates predictions via prior class probabilities in the training set.

Average MRC-I score: We consider the imageability scores of 3,769 words in the MRC lexicon and normalize them to be $\in [0, 1]$. For each example, we take the average of the imageability scores of the unique words; out-of-vocabulary words are assigned a score of 0. We lowercase the words in the MRC lexicon as well as the input text. Based on this average score, we categorize an example as either `visual` or `non-visual` by setting the decision boundary as 0.17. The threshold is chosen to optimize the performance on the validation set of TIMED.

Concentration of Visual Genome Objects (VG-Objects): The Visual Genome dataset comprises 75,729 objects, along with annotations for their attributes and object-object relations (Krishna et al. 2017). Based on the heuristic that a mention of a visual object in the text can trigger imageability, we quantify the concentration of Visual Genome objects by computing the fraction of unique object mentions in tokenized text with respect to the number of total unique words within the input text. We set the threshold to 0.5 based on the performance on the validation set.

Expanding the MRC lexicon using word embeddings: The coverage of the MRC lexicon is poor because it contains only 3,769 words. We expand the list of word-level human-assigned imageability scores using semantic similarity between distributed representations of words.[4] For each word w in the word2vec (Mikolov et al. 2013) vocabulary of pre-trained representations that does not occur in the MRC lexicon, we compute its cosine similarities with all the words in the MRC lexicon to identify the most semantically similar word that exists in MRC, given by w_{MRC} and its similarity with w given as (sim_{max}). We assign the word w an imageability score of $sim_{max} \times score_{w_{\text{MRC}}}$, where $score_{w_{\text{MRC}}}$ is the normalized imageability score of w's most similar word w_{MRC}. Based on the performance on the validation set, the decision boundary for average imageability score of input text is set as 0.17. This baseline propagation approach is highly effective in quantifying word-level imageability as the Pearson's correlation coefficient between the assigned visualness score and the average AMT rating of humans is $0.735 (p < 0.001)$; see Appendix 8.2 for details.

Fine-tuned BERT classifier: We fine-tune a BERT model (`bert-base-uncased` on HuggingFace (Devlin et al. 2018; Wolf et al. 2020)) for the binary classification task of `visual` versus `non-visual` text detection. Similar to our proposed model, we adopt a two-stage fine-tuning approach with the BERT classifier (adding a classification layer to BERT for the first input token's (`[CLS]`) representation). We first fine-tune the model using the automatically labeled dataset followed by fine-tuning on the training set of the human-curated TIMED. For the first stage, we fine-tune the model for 7 epochs with a learning rate initialized at 5×10^{-5} using a batch size of 32 while setting other hyperparameters to default. We fine-tune the model for 3 epochs for the second stage with the same hyperparameters (chosen based on the performance on TIMED validation set).

[4] We experiment with 300-dim word2vec vectors trained on the Google News corpus, comprising 3M words and phrases.

MODELS	$F_1 \uparrow$	PRECISION ↑	RECALL ↑	ACC. ↑
Random	0.531	0.531	0.531	0.577
MRC-I	0.584	0.599	0.583	0.644
VG-Objects	0.606	0.610	0.605	0.646
MRC-I + w2v	0.638	0.637	0.639	0.667
BERT	0.753	0.766	0.789	0.756
CLIP	0.694	0.695	0.701	0.712
TIP-CLIP (Ours)	**0.865**	**0.858**	**0.873**	**0.871**

Table 2: Evaluation on human-annotated test set of TIMED. Reported F_1, Precision, and Recall values are macro-averages across the two classes (`visual` and `non-visual`).

Pre-trained CLIP model: We use the pre-trained CLIP model (ViT/B-32) to obtain similarity scores between the embeddings of the `NULL` image (used for the fine-tuning of our model) and the input text. We then use $1 - \langle I^e_{\texttt{NULL}}, T^e \rangle$ as an estimate of the visual score of text (see Eq. 3). Based on the performance on the TIMED validation set, we set the threshold for $\mathcal{S}$ to be 0.83.

6 Results and Analyses

Evaluation on held-out test set of TIMED: We first evaluate the baselines and our approach on the test set of the human-annotated TIMED, computing macro-averaged F_1, precision, recall scores, and classification accuracy. Table 2 show the results for this evaluation. We observe that our proposed two-stage fine-tuning strategy leads to the best-performing model (TIP-CLIP). In comparison, the pre-trained CLIP model demonstrates notably weaker performance on the task of distinguishing visual text from non-visual text. Interestingly, fine-tuned BERT performs reasonably well on the task, considerably better than the CLIP model. Using the average imageability scores from MRC provides better-than-random performance but is severely subpar to models like CLIP, BERT, and TIP-CLIP. Using word2vec embeddings to expand the coverage of the MRC lexicon (i.e., MRC-I + w2v) leads to a boost in performance. However, collectively, the lacking performance of MRC-I and MRC-I + w2v demonstrates that word-level imageability does not translate to sentence-level imageability to a great extent. Notably, in terms of baselines that aggregate word-level attributes, VG-Objects provides the best estimate of sentence-level imageability by quantifying the concentrations of visual objects in the input sentence.

Correlation of Attention Weights with MRC Imageability Scores: Attention mechanisms could be taken as proxies for explainability (Wiegreffe and Pinter 2019; Chefer, Gur, and Wolf 2021). Since the fine-tuned BERT, pre-trained CLIP, and our TIP-CLIP are attention-based models, we compute the correlation between average word-level attention scores (obtained from the last layer) on a given dataset with the imageability scores assigned by humans in the MRC lexicon. We compute these values for two datasets—the MSCOCO dataset (Vinyals et al. 2016) and

MODELS	MSCOCO	TIMED
BERT	0.461*** (n = 344)	0.326*** (n = 294)
CLIP	0.448*** (n = 344)	0.283*** (n = 294)
TIP-CLIP (Ours)	**0.497***** (n = 344)	**0.367***** (n = 294)

Table 3: Correlation between MRC Imageability scores and model attention-scores for BERT, CLIP, and TIP-CLIP. n denotes the number of overlapping words across vocabularies; *** denotes $p < 10^{-3}$.

MODELS	$F_1 \uparrow$	PRECISION $\uparrow$	RECALL $\uparrow$	ACC. $\uparrow$
BERT (auto-labeled)	0.714	0.704	0.716	0.710
BERT (human-labeled)	0.753	0.766	0.789	0.756
BERT (auto + human-labeled)	0.774	0.783	0.797	0.771
CLIP	0.694	0.695	0.701	0.712
TIP-CLIP (auto-labeled)	0.751	0.763	0.791	0.748
TIP-CLIP (human-labeled)	0.810	0.807	0.815	0.820
TIP-CLIP (auto + human-labeled)	**0.865**	**0.858**	**0.873**	**0.871**

Table 4: Ablation studies to understand the benefits of two-stage fine-tuning. The presented results are on the human-annotated test set of TIMED. Reported values are macro-averages of class-wise F_1, precision, and recall, and overall classification accuracy.

the test set of TIMED. We only consider words that occur more than once in the specific corpus. Table 3 shows that TIP-CLIP attention scores correlate the most with MRC imageability scores, followed by the fine-tuned BERT's attention scores. The trends are consistent across both datasets. The relative ordering of models in terms of the correlation of their attention scores with MRC imageability scores follows the same order as their performance on the test set of TIMED. However, all correlation scores are in the low range, indicating a non-trivial relationship between sentence- and word-level imageability.

The same trends hold for propagated visualness scores, albeit with slightly lower values of the correlation scores (see Appendix 8.4). We also analyze the reason behind higher correlation scores on MSCOCO with respect to the TIMED corpus in Appendix 8.4.

Effect of multi-stage training: We conduct ablations to isolate the effect of two-stage training. In Table 4, we show that BERT and TIP-CLIP can learn to distinguish `visual` and `non-visual` text even when fine-tuned only using the automatically labeled data. However, for both models, the gains from fine-tuning only on smaller, human-labeled data are notably higher. Furthermore, we find the proposed two-stage fine-tuning (i.e., training on automatically labeled data followed by human-labeled data) to be most effective, leading to a gain of over 2 and 5 absolute F_1 points over training only on human-labeled data for BERT and TIP-CLIP models, respectively. Additionally, for a given training strategy, our proposed fine-tuning of TIP-CLIP demonstrates better performance than the corresponding fine-tuned BERT model as well as the standard pre-trained CLIP model.

Effect on Text-to-Image Retrieval: We aim to analyze the re-usability of learned embeddings by the TIP-CLIP model for the text-to-image retrieval task. To this end, we consider the 515 `visual` examples from the test set of TIMED and, for each `visual` example, we rank the 515 corresponding images based on the cosine similarity between the image and text embeddings obtained from the TIP-CLIP model. We compute the Mean Reciprocal Rank (MRR) and contrast it with the MRR obtained using the pre-trained CLIP embeddings. As expected, CLIP achieves a near-perfect MRR of 0.989. The proposed fine-tuning objective does not severely impact the reusability of embeddings obtained from TIP-CLIP for retrieval, and results in an MRR of 0.937. This comparison evaluates the retrieval capabilities of TIP-CLIP against that of the CLIP model because the correspondence between visual text and images was established using similarities between CLIP embeddings.[5]

The downside of an alternate training objective: Recall that our fine-tuning strategy involves matching `visual` text with its corresponding image and matching `non-visual` text with the `NULL` image. With only the classification of `visual` and `non-visual` text in mind, an alternate fine-tuning strategy would have been to match all the `visual` examples with one common image while matching all the `non-visual` text with the common `NULL` image. The major downside of this approach is that while it leads to an effective classifier after two-stage fine-tuning, demonstrating a comparable F_1 score of 0.842 as the TIP-CLIP model, it performs poorly on the text-to-image retrieval task with an MRR of 0.014. Overall, while the alternate entirely classification-based training objective performs at par with the proposed TIP-CLIP model on the classification task, the resultant embeddings demonstrate poor reusability for downstream tasks like text-to-image retrieval.

Properties of the new embedding space: In Figure 2 we visualize the embedding space of the learned embeddings using t-SNE (Van der Maaten and Hinton 2008). Alongside `visual` and `non-visual` sentences from the test set of TIMED, we also plot the embeddings of images corresponding to the `visual` sentences, and the embedding(s) of the `NULL` image(s). First off, we observe that the embeddings in Figure 2a and 2b from CLIP and TIP-CLIP are different in that the TIP-CLIP embeddings demonstrate better distinguishability between `visual` and `non-visual` text. In Figure 2c we observe that the alternative formulation pushes the `NULL` embeddings to the periphery of the image embeddings' cluster from a near-center location in Figures 2a and 2b. The text embeddings demonstrate notable distinguishability in Figure 2c too. We believe that the alternative classification-only formulation causes distortion in the latent space that causes drastic modification of text-only embeddings, making them useless for downstream text-to-image retrieval, as demonstrated empirically earlier. However, our proposed objective in TIP-CLIP preserves reusability for downstream tasks by maintaining semantic relevance between learned image and text embeddings.

6.1 Qualitative Analysis

In this section we conduct two qualitative analyses: *(i)* contrasting the attention mechanisms for CLIP and TIP-

[5]While establishing the correspondence between `visual` text and images, we enforce the constraint that the most similar image for a text should exist on the same page of the PDF. Therefore, it is possible that while ranking all the images in the test set, the CLIP similarity of text may be higher for a different image, resulting in an MRR slightly less than 1.0 (i.e., 0.989).

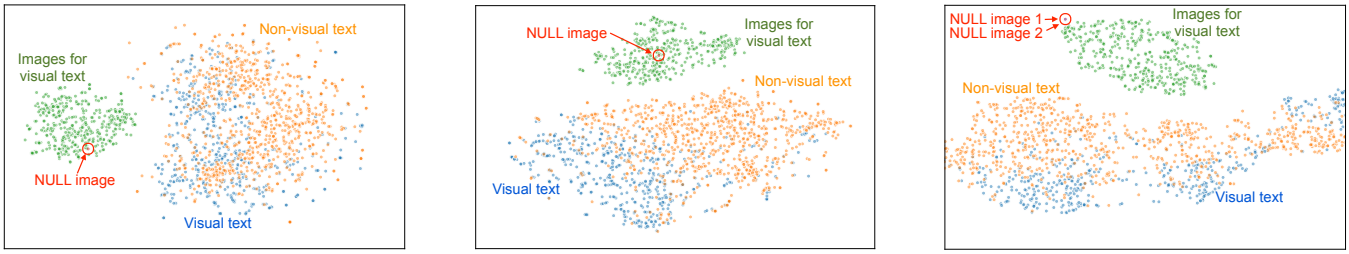

(a) CLIP embeddings (b) TIP-CLIP embeddings (c) Alt. formulation embeddings

Figure 2: t-SNE visualization of embeddings learned by (a) CLIP, (b) TIP-CLIP — using contrastive and adapted contrastive learning objective, respectively, & (c) model trained using alternative formulation solely focusing on classification. The plotted data points are from the TIMED test set.

CLIP, and *(ii)* the role of distinguishing `visual` and `non-visual` text in downstream text-to-image generation using systems like DALL-E (Ramesh et al. 2021b).

Attention Map Visualization: To contrast the mechanism by which CLIP and TIP-CLIP models match input text with their corresponding image, we visualize and contrast the attention maps for both models. We adopt the state-of-the-art approach to explain multimodal Transformers (Chefer, Gur, and Wolf 2021). In Appendix Figure 3 we show 4 illustrative `visual` sentences from the test set of TIMED along with their corresponding images. Focusing on text, we observe that TIP-CLIP has a greater tendency to attend to visual aspects in the text; for instance, words like 'christmas,' 'islands,' 'lakes,' 'anglers' are attended to a greater extent by TIP-CLIP than CLIP. In images, we observe small changes in attention maps across CLIP and TIP-CLIP; for instance, while the CLIP attention is focused on the Common Loon, TIP-CLIP also attends to the 'lake.' It is worth noting that the proposed fine-tuning objective that TIP-CLIP follows is closely related to the original contrastive objective for training CLIP – both encourage the matching of correct image-text pairs for `visual` sentences *but* TIP-CLIP additionally encourages matching of `non-visual` text to the `NULL` image. The qualitative analysis of visualization maps reinforces that the matching process for text and images undergoes small changes to accommodate for greater attention to visual aspects in the text.

Downstream Text-to-Image Generation: In Appendix Fig. 4 we show the generations obtained using DALL-E for text that is categorized as `non-visual` and `visual` in our dataset. We observe that for `non-visual` text, the images produced by DALL-E show poor relevance to the text. However, for `visual` text the generated images demonstrate great relevance to the input text. Qualitatively, if the text contains declarative information, DALL-E generates text-heavy images (last two examples in Appendix Fig. 4(a)). For `visual` text, we observe that visual concepts like 'melted snow on grass,' 'Tai chi,' 'joggers in the garden,' and 'running in a race, are well represented in the generated images.

Triggering image-to-text generation models like DALL-E for the text that is identified as visual is crucial to effectively use such systems in a passive setting. For instance, while working with long-form documents, the authors should only be recommended to add visual assets in relevant places (i.e., for visual sentences). Triggering image generations for non-visual sentences could cause suboptimal user experiences by recommending irrelevant images. To this end, our contributions focus on distinguishing visual text from non-visual text as the necessary first step.

TIP-CLIP also demonstrates the best out-of-domain (Twitter) generalizability compared to the baselines considered here; see Appendix 8.5 for more details. We also analyze the predictions of competitive models on the `ambiguous` sentences in TIMED in Appendix 8.6.

7 Conclusion and Future Work

We propose the task of predicting the visualness of text and curate a human-annotated dataset of sentence-level visualness scores. Additionally, we propose a two-stage fine-tuning objective for the task that involves training on a distantly supervised corpus followed by a smaller human-annotated corpus. Comparisons with several baselines demonstrate the effectiveness of our approach in distinguishing visual and non-visual text. Furthermore, analyses of attention weights for our model indicate a greater correlation with word-level imageability scores than other attention-based baselines. The embeddings from our approach are transferable to downstream text-to-image retrieval. Qualitative analysis of attention weights over textual input reinforces that our model attends to visual words to a greater extent. In closing, we show qualitative examples of how predicting text visualness can make text-to-image generation more targeted and effective.

In future, we aim to study alternate objectives for learning text visualness while ensuring transferable representations for more downstream tasks. As the aggregation of word-level visualness scores leads to poor predictability of sentence-level visualness, future work could aim to understand the compositionality in language that precipitates visualness at the sentence level. Additionally, we will study in detail how text visualness impacts the quality and relevance of images generated using systems like DALL-E.

References

Antol, S.; Agrawal, A.; Lu, J.; Mitchell, M.; Batra, D.; Zitnick, C. L.; and Parikh, D. 2015. Vqa: Visual question answering. In *CVPR*.

Baltrušaitis, T.; Ahuja, C.; and Morency, L.-P. 2018. Multimodal machine learning: A survey and taxonomy. *IEEE PAMI*.

Bird, S. 2006. NLTK: the natural language toolkit. In *COLING/ACL*.

Chefer, H.; Gur, S.; and Wolf, L. 2021. Generic attention-model explainability for interpreting bi-modal and encoder-decoder transformers. In *ICCV*.

Chen, Y.-C.; Li, L.; Yu, L.; El Kholy, A.; Ahmed, F.; Gan, Z.; Cheng, Y.; and Liu, J. 2020. Uniter: Universal image-text representation learning. In *ECCV*. Springer.

Coltheart, M. 1981. The MRC psycholinguistic database. *The Quarterly Journal of Exp. Psyc.*

Deschacht, K.; and Moens, M. F. 2007. Text analysis for automatic image annotation. In *ACL*.

Devlin, J.; Chang, M.-W.; Lee, K.; and Toutanova, K. N. 2018. BERT: Pre-training of Deep Bidirectional Transformers for Language Understanding.

Goodfellow, I. J.; Mirza, M.; Xiao, D.; Courville, A.; and Bengio, Y. 2013. An empirical investigation of catastrophic forgetting in gradient-based neural networks. *arXiv preprint: 1312.6211*.

Jeong, J.-W.; Wang, X.-J.; and Lee, D.-H. 2012. Towards measuring the visualness of a concept. In *CIKM*.

Jia, C.; Yang, Y.; Xia, Y.; Chen, Y.-T.; Parekh, Z.; Pham, H.; Le, Q.; Sung, Y.-H.; Li, Z.; and Duerig, T. 2021. Scaling up visual and vision-language representation learning with noisy text supervision. In *ICML*. PMLR.

Karpinska, M.; Akoury, N.; and Iyyer, M. 2021. The Perils of Using Mechanical Turk to Evaluate Open-Ended Text Generation. In *EMNLP*.

Kingma, D. P.; and Ba, J. 2014. Adam: A method for stochastic optimization. *arXiv preprint: 1412.6980*.

Krishna, R.; Zhu, Y.; Groth, O.; Johnson, J.; Hata, K.; Kravitz, J.; Chen, S.; Kalantidis, Y.; Li, L.-J.; Shamma, D. A.; et al. 2017. Visual genome: Connecting language and vision using crowdsourced dense image annotations. *IJCV*.

Long, M.; Cao, Y.; Wang, J.; and Jordan, M. 2015. Learning transferable features with deep adaptation networks. In *ICML*.

Louis, A.; and Nenkova, A. 2013. What makes writing great? First experiments on article quality prediction in the science journalism domain. *TACL*.

Lu, J.; Batra, D.; Parikh, D.; and Lee, S. 2019. Vilbert: Pretraining task-agnostic visiolinguistic representations for vision-and-language tasks. *NeurIPS*.

Mikolov, T.; Sutskever, I.; Chen, K.; Corrado, G. S.; and Dean, J. 2013. Distributed representations of words and phrases and their compositionality. *NeurIPS*.

Miller, G. A. 1995. WordNet: A Lexical Database for English. *Comm. ACM*, 38(11): 39.

Mittal, A.; Dahiya, K.; Malani, S.; Ramaswamy, J.; Kuruvilla, S.; Ajmera, J.; Chang, K.-h.; Agarwal, S.; Kar, P.; and Varma, M. 2022. Multi-modal Extreme Classification. In *CVPR*.

Paivio, A.; Yuille, J. C.; and Madigan, S. A. 1968. Concreteness, imagery, and meaningfulness values for 925 nouns. *Journal of Exp. Psych.*

Pennington, J.; Socher, R.; and Manning, C. D. 2014. Glove: Global vectors for word representation. In *EMNLP*.

Radford, A.; Kim, J. W.; Hallacy, C.; Ramesh, A.; Goh, G.; Agarwal, S.; Sastry, G.; Askell, A.; Mishkin, P.; Clark, J.; et al. 2021. Learning transferable visual models from natural language supervision. In *ICML*, 8748–8763. PMLR.

Ramesh, A.; Dhariwal, P.; Nichol, A.; Chu, C.; and Chen, M. 2022. Hierarchical text-conditional image generation with clip latents. *arXiv preprint: 2204.06125*.

Ramesh, A.; Pavlov, M.; Goh, G.; Gray, S.; Voss, C.; Radford, A.; Chen, M.; and Sutskever, I. 2021a. Zero-shot text-to-image generation. In *ICML*. PMLR.

Ramesh, A.; Pavlov, M.; Goh, G.; Gray, S.; Voss, C.; Radford, A.; Chen, M.; and Sutskever, I. 2021b. Zero-shot text-to-image generation. In *ICML*. PMLR.

Rombach, R.; Blattmann, A.; Lorenz, D.; Esser, P.; and Ommer, B. 2022. High-resolution image synthesis with latent diffusion models. In *CVPR*.

Saharia, C.; Chan, W.; Saxena, S.; Li, L.; Whang, J.; Denton, E.; Ghasemipour, S. K. S.; Ayan, B. K.; Mahdavi, S. S.; Lopes, R. G.; et al. 2022. Photorealistic Text-to-Image Diffusion Models with Deep Language Understanding. *arXiv preprint: 2205.11487*.

Sarto, S.; Cornia, M.; Baraldi, L.; and Cucchiara, R. 2022. Retrieval-Augmented Transformer for Image Captioning. *arXiv preprint: 2207.13162*.

Srinivasan, K.; Raman, K.; Chen, J.; Bendersky, M.; and Najork, M. 2021. WIT: Wikipedia-based Image Text Dataset for Multimodal Multilingual Machine Learning. *arXiv preprint: 2103.01913*.

Tan, H.; and Bansal, M. 2019. LXMERT: Learning Cross-Modality Encoder Representations from Transformers. In *EMNLP-IJCNLP*.

Van der Maaten, L.; and Hinton, G. 2008. Visualizing data using t-SNE. *JMLR*.

Vinyals, O.; Toshev, A.; Bengio, S.; and Erhan, D. 2016. Show and tell: Lessons learned from the 2015 mscoco image captioning challenge. *IEEE PAMI*.

Wang, K.; Yin, Q.; Wang, W.; Wu, S.; and Wang, L. 2016. A comprehensive survey on cross-modal retrieval. *arXiv preprint: 1607.06215*.

Wiegreffe, S.; and Pinter, Y. 2019. Attention is not not Explanation. In *EMNLP-IJCNLP*.

Wolf, T.; Debut, L.; Sanh, V.; Chaumond, J.; Delangue, C.; Moi, A.; Cistac, P.; Rault, T.; Louf, R.; Funtowicz, M.; et al. 2020. Transformers: State-of-the-art natural language processing. In *EMNLP (System Demonstrations)*.

Xu, K.; Ba, J.; Kiros, R.; Cho, K.; Courville, A.; Salakhudinov, R.; Zemel, R.; and Bengio, Y. 2015. Show, attend and tell: Neural image caption generation with visual attention. In *ICML*. PMLR.

Yosinski, J.; Clune, J.; Bengio, Y.; and Lipson, H. 2014. How transferable are features in deep neural networks? *NeurIPS*.

Yuan, X.; Lin, Z.; Kuen, J.; Zhang, J.; Wang, Y.; Maire, M.; Kale, A.; and Faieta, B. 2021. Multimodal Contrastive Training for Visual Representation Learning. In *CVPR*.

8 Appendix

8.1 Effect of the NULL Image

Since all the non-visual sentences in the training corpus are mapped to a common NULL image, we aim to see the effect of the chosen NULL image on the results. Recall that the NULL image used for our main experiments was obtained by creating an RGB image in which each pixel value is chosen randomly. We perform the same process with a different random seed to generate another NULL image. Additionally, we use a natural image as another alternative for the NULL image. These images are shown in Figure 5. We then evaluate the resulting models on the human-annotated test set of TIMED. Table 5 shows that the performance of the models is not dependent on the choice of the NULL image. We also find no dependence between the choice of the NULL image and the performance on downstream text-to-image retrieval.

8.2 Assessment of word-level imageability score propagation

We randomly selected 500 words from the MRC lexicon and 500 words from the word2vec vocabulary that did not occur in the MRC lexicon. Each word was shown to 9 annotators using Amazon Mechanical Turk to seek responses to the following question: "*Do you agree that the word below evokes an image or picture in your mind?*" The annotators were instructed to respond on a 7-point Likert scale, where 1 denoted strong disagreement and 7 denoted strong agreement. Please see Appendix 8.3 for details about the instructions, demographic filters, and compensation.

We average the ratings for all the annotated words and normalized them to be $\in [0, 1]$. We compute the Pearson's correlation coefficient between *(a)* the average ratings for MRC words and the normalized imageability scores, and *(b)* the average ratings for word2vec words and the imageability scores assigned via embedding-based propagation. The correlation between MRC imageability scores and average annotators' ratings is 0.870 ($p < 0.001$) and the correlation between scores assigned via our propagation method and average annotators' ratings is 0.735 ($p < 0.001$). This high positive correlation coefficient between assigned imageability scores and human-perceived ratings demonstrates the effectiveness of our adopted propagation method. We also note that the inter-annotator agreements for the ratings for MRC words and word2vec words, as computed using Krippendorf's α (ordinal measure), were 0.626 and 0.584, respectively.

Overall, this assessment illustrates the validity of propagating word-level imageability scores using embedding-based semantic similarities. More broadly, the aim of adopting this approach is to expand the coverage of MRC lexicon. Qualitatively, we observe that words like 'gotcha' (0.33) and 'presbyterian' (0.61) are assigned meaningful imageability scores, demonstrating expansion along time and domains. As a point of difference between human ratings and assigned scores, we notice that the propagation approach assigned a high imageability score to words like 'qawwali' (0.60) while the human annotators did not, possibly due to lacking sociocultural context. In Table 6 we show illustrative words that are assigned high (≥ 0.7), medium ($\in (0.3, 0.7)$), and low (≤ 0.3) imageability scores using our propagation method.

8.3 Details about MTurk Experiments

For all our annotation tasks, we recruited annotators using Amazon Mechanical Turk. We set the criteria to 'Master' annotators with at least a 99% approval rate and were located in the United States. To further ensure the quality of annotations, we required the annotators to have at least 5000 accepted annotations in the past. The rewards were set by assuming an hourly rate of 12 USD for all the annotators. We show the annotation interfaces in Figure 6.

For our human evaluations, we also inserted some "attention-check" examples during the annotation tasks to ensure the annotators read the text carefully before responding. This was done by asking the annotators to mark a randomly-chosen score on the Likert scale regardless of the actual content. We discard the annotations from annotators who did not correctly respond to all the attention-check examples and re-collect annotations for the affected samples.

8.4 Further analyses on the correlation between attention scores and word-level visualness scores

We compute the Pearson's correlation coefficient between a model's average attention scores over words and the visualness score assigned using our propagation method. However, unlike Table 3, this time, we consider the propagated imageability scores which lead to broader coverage in terms of vocabulary. As seen in Table 7, we observe the same trends as with MRC imageability scores, albeit with slightly lower values of correlation scores.

To analyze the alignment between learned attention scores for various models, we compute the correlation between average attention scores across different models. Pearson's correlation coefficients in Table 8 show that all the model attention scores have a moderate correlation with each other.

Why are correlation scores higher for MSCOCO than for TIMED?: An interesting trend across Table 3 and 7 is that the correlation scores are consistently higher, across all the models under consideration, for the MSCOCO dataset than the test set of TIMED. We note that, on average, MSCOCO has a caption length of 11.4 whereas the TIMED dataset has an average sentence length of 20.6, with a greater concentration of objects from the Visual Genome objects—6.7 (58.7%) objects per example versus 8.4 (40.7%) objects per example). For our TIP-CLIP model, these objects acquire an average of 63.2% attention scores across all the MSCOCO examples, whereas they only acquire 37.1% of attention scores, on average, across the examples in the TIMED test set. Overall, these results demonstrate that the TIP-CLIP model attends over words in the MSCOCO corpus in an object-targeted manner but the attention is relatively diffused in the TIMED corpus. Combined with the observation that MRC imageability scores are higher for concrete objects (Paivio, Yuille, and Madigan 1968), this explains why the correlation scores are consistently higher on MSCOCO than on TIMED.

Effect of length on the correlation between attention and MRC-I scores: We categorize the sentences in the test set of

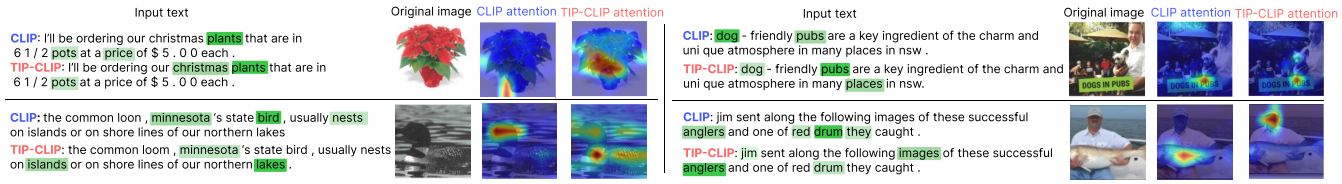

Figure 3: Comparing the attention maps over input text and images for CLIP and TIP-CLIP. For text, a darker shade of green demonstrates greater attention by the model. For images, red demonstrates the greatest attention in the heatmap. Image best viewed with zoom.

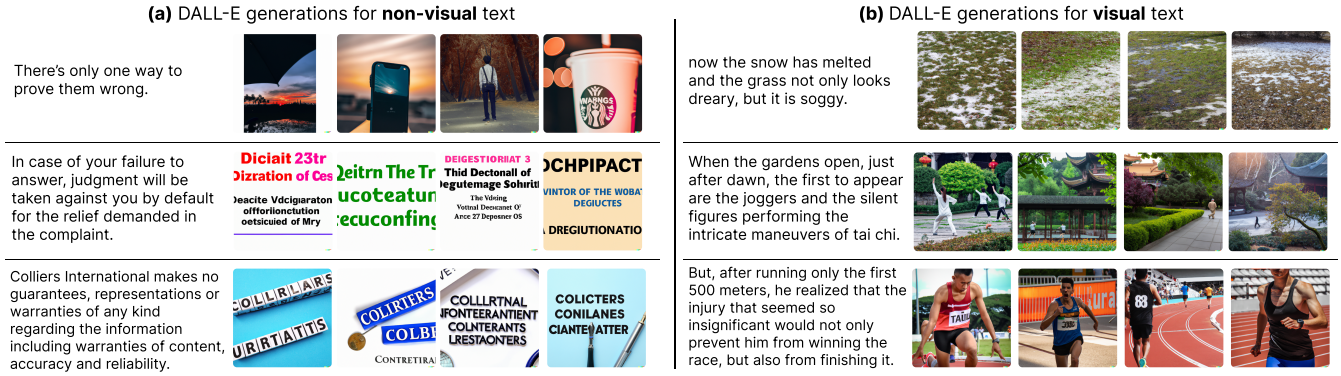

Figure 4: Examples of DALL-E generations for `non-visual` and `visual` text.

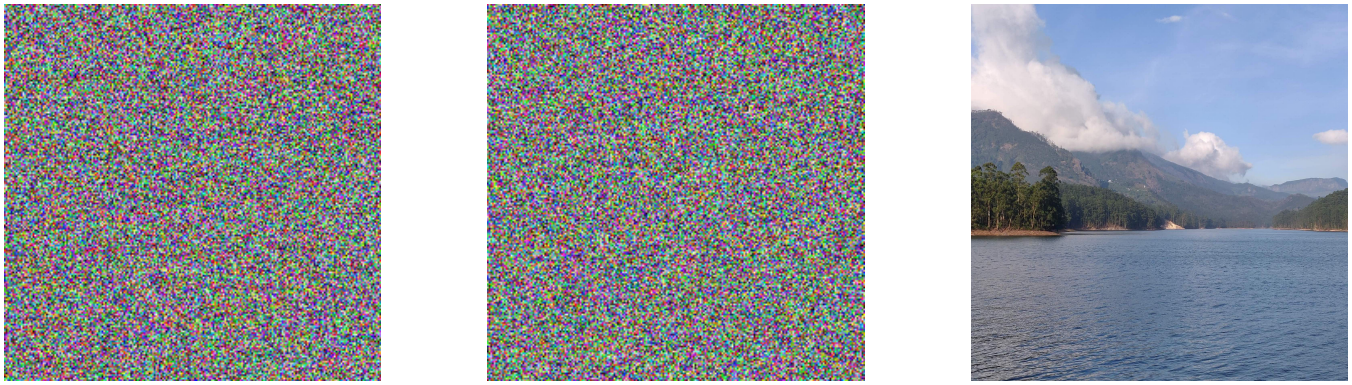

(a) Original `NULL` image (b) `NULL` image with diff. seed (c) Natural `NULL` image

Figure 5: Various `NULL` images used to study the effect of the chosen image on the text visualness identification task and the downstream text-to-image retrieval task.

VARIANTS	$F_1 \uparrow$	PRECISION ↑	RECALL ↑	ACC. ↑	MRR ↑
TIP-CLIP (Original – Fig. 5a)	0.865	0.858	0.873	0.871	0.937
TIP-CLIP (w/ diff. seed – Fig. 5b)	0.867	0.854	0.875	0.872	0.934
TIP-CLIP (natural image - Fig. 5c)	0.861	0.855	0.876	0.872	0.939

Table 5: Effect of the choice of the `NULL` image on categorizing the human-annotated test set of TIMED and downstream text-to-image retrieval. Reported F_1, Precision, and Recall values are macro-averages across the two classes (`visual` and `non-visual`).

TIMED into short (≤ 10; $n = 304$), medium ($\in (10, 20)$; $n = 505$), and long (≥ 20; $n = 606$) sentences based on word counts. However, we did not find a notable variation in the correlation scores between the attention weights of the TIP-CLIP model and MRC Imageability scores. Pearson's correlation coefficient was 0.33, 0.35, and 0.37 for short,

Category	Example words (assigned score)
High imageability	martini, crabmeat, teeth, oysters, mosquitos, bracelets, motorboat, diamonds, squirrels, cigarettes, beaches, trumpets, dolphin, caramel, cattle, portobello, libraries, chimpanzee, snorkeling, sailboat, harmonica
Medium imageability	reassure, militancy, inhumanly, catalyses, industrial, peacefulness, handwoven, neurosurgery, overwashed, whooper, snails, preeminence, recluse, entrepreneur, character, insufficient, paladin, impersonal, deviously, recover
Low imageability	politologist, psycholinguistic, requirements, confirmatory, terseness, preformulation, offender, controversial, unhealable, monoculturalism, miserable, reprogrammability, this, participate, attractive, determinant, disestablishment

Table 6: Qualitative examples of words that are assigned scores in the high (≥ 0.7), medium ($\in (0.3, 0.7)$), and low (≤ 0.3) range using the word2vec embedding-based propagation methodology.

MODELS	MSCOCO	TIMED
BERT	0.434***	0.301***
CLIP	0.429***	0.262***
TIP-CLIP (Ours)	**0.465****	**0.338****

Table 7: Pearson's correlation coefficient between propagated imageability scores (using word2vec) and model attention-scores. *** denotes $p < 0.001$

medium, and long sentences, respectively. We observed the same trend for the fine-tuned BERT model and the pre-trained CLIP model.

MODELS	BERT	CLIP	TIP-CLIP
BERT	—	–	–
CLIP	0.552***	–	–
TIP-CLIP (Ours)	0.631***	0.571***	–

Table 8: Pearson's correlation coefficient between word-level attention scores of various models for the TIMED test set. *** denotes $p < 0.001$

8.5 Out-of-Domain Generalization

MODELS	$F_1 \uparrow$	PRECISION ↑	RECALL ↑	ACC. ↑
Random	0.503	0.503	0.503	0.505
MRC-I	0.470	0.472	0.472	0.470
VG-Objects	0.536	0.541	0.539	0.548
MRC-I + w2v	0.501	0.502	0.504	0.502
MRC-I + GloVe (Twitter)	0.516	0.518	0.520	0.519
BERT	0.612	0.634	0.624	0.618
CLIP	0.644	0.645	0.645	0.644
TIP-CLIP (Ours)	**0.696**	**0.693**	**0.691**	**0.694**

Table 9: Out of domain evaluation on the Twitter dataset. Reported F_1, Precision, and Recall values are macro-averages across the two classes (`visual` and `non-visual`).

A critical assessment of the robustness and generalizability of the models trained using our proposed approach is to conduct evaluations on out-of-domain (OOD) datasets. To this end, we curate a social media dataset by scraping Twitter. We start with the Wikipedia-based Image Text Dataset (WIT) (Srinivasan et al. 2021) and query Twitter using the Wikipedia page title to retrieve posts in English that are *with* and *without* images. We require that the retrieved post contains the page title string to ensure topical similarity between posts with and without images. To remove examples with irrelevant images, we discard posts with a CLIP-similarity lower than 0.70 between the Twitter post's image and the corresponding image on Wikipedia. Consequently, we obtain a dataset of Twitter posts containing mentions of 1185 Wikipedia topics, 7844 Twitter posts with images, and 7248 Twitter posts without images. The posts with and without images are tied by common Wikipedia topics.

We hypothesize that the text in Twitter posts that mention a certain topic and contain an image are more visual than text in Twitter posts that mention the same topic and do not contain any images. To test this hypothesis, we randomly sample 40 Wikipedia topics and present the associated text with ($n = 264$) and without images ($n = 241$) to human annotators. In an AMT survey that follows the design for curating TIMED, we find that the average annotator rating for the text from Twitter posts *without* images is 2.306 (± 1.369) while that for text from Twitter posts *with* images is 4.304 (± 1.273). We observe the inter-annotator agreement of 0.413, which is similar to that observed while curating TIMED. For 34 out of the 40 Wikipedia topics, the annotators provided a higher imageability rating to text originally associated with an image on Twitter than text not associated with an image. Overall, the AMT survey validates our hypothesis by demonstrating that text in Twitter posts with images is perceived as more visual than text in Twitter posts without images, modulo the topic is common across the posts.

We now ask the question: how well the models considered in our work categorize Twitter text with images as `visual` and Twitter text without images as `non-visual`? We first adapt the thresholds used to classify text using various methods by running an evaluation on a randomly sampled validation set of 100 Twitter examples, 50 from each category. The thresholds are set as follows: MRC-I: 0.19; VG-Objects: 0.52; MRC-I + w2v: 0.17; MRC-I + GloVe: 0.32[6]; CLIP:

[6]Since we are operating with the Twitter domain, we design a version of the propagation method where MRC Imageability

(a) Interface to collect sentence-level visualness scores

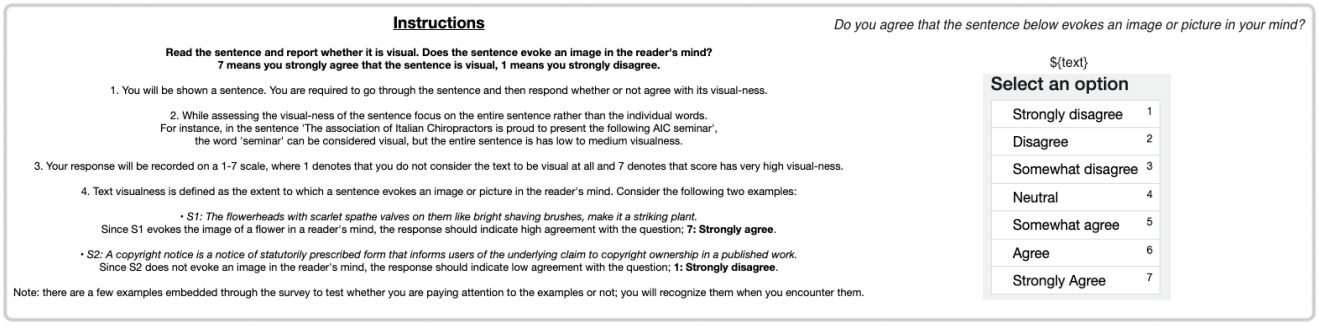

(b) Interface to evaluate word-level visualness scores assigned by the propagation method

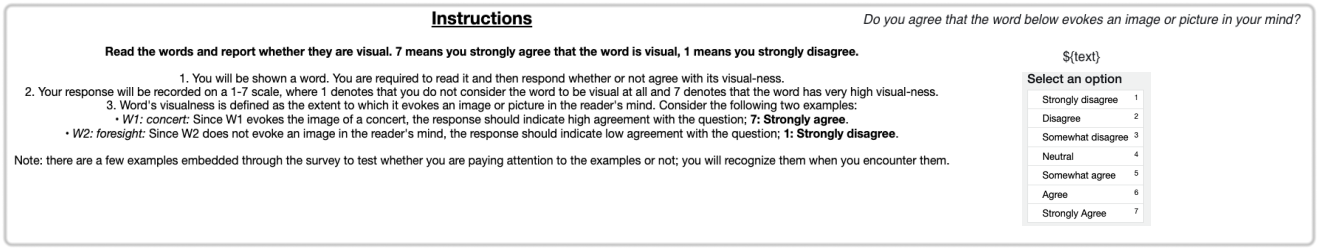

Figure 6: Interface for our annotation tasks on Amazon Mechanical Turk. For each of the annotations task, we also show the instructions provided to the annotators.

0.87; TIP-CLIP: 0.74. Using these threshold values, we categorize the rest of the Twitter dataset ($n = 14,992$) into visual and non-visual categories. The random baseline uses uniform sampling.

Table 9 shows the results for this out-of-domain evaluation. First, we note that all models undergo a severe drop in performance on the OOD dataset, indicating that the notion of sentence-level imageability is strongly tied to the domain. Our proposed TIP-CLIP model demonstrates better OOD generalization capabilities than all the considered baselines. It is noteworthy that the fine-tuned BERT model performs poorly on the OOD dataset than the standard pre-trained CLIP model. The aggregation of word-level imageability scores provides a worse-than-random estimate of sentence-level imageability on the OOD dataset.

8.6 Predictions on Ambiguous Sentences

Recall that while curating TIMED, we combined examples without a clear majority from the annotators ($n = 378$) and those with majority votes for the 'Neutral' category ($n = 2$) into a single category called `ambiguous`. We revisit these examples to analyze how the most-competitive baselines and our proposed TIP-CLIP model score them on imageability. We compute the imageability score using Equation 3 for CLIP and TIP-CLIP, while treating fine-tuned BERT's prediction probability score as its imageability score for a given example. To appropriately compare the distribution of imageability scores across these three models, we standardize the values by computing z-scores (i.e., x_i is transformed into $z_i = (x_i - \mu)/\sigma$; where x_i is the original value, μ and σ are mean and standard deviation of the distribution that x_i belongs to). In Figure 7, we show that while CLIP and TIP-CLIP imageability scores are distributed normally around their respective means, BERT imageability scores are bimodal with peaks close to one standard deviation away from

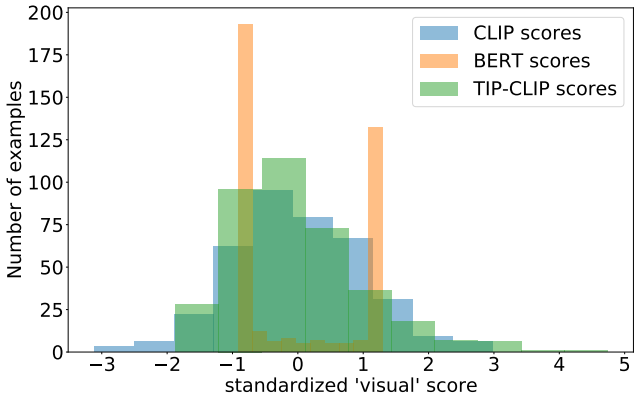

Figure 7: Distribution of standardized visualness scores for ambiguous examples (i.e., $(v - \mu)/\sigma$, where v is the original visualness score, μ and σ are the mean and standard deviation of the distributions, respectively). We contrast the predicted visualness scores by fine-tuned BERT, pre-trained CLIP, and our TIP-CLIP models.

scores are propagated in the GloVe-embedding space, where the GloVe embeddings are learned on Twitter corpus (Pennington, Socher, and Manning 2014). We use 200-dimensional GloVe vectors trained on 2 billion Twitter posts with a vocabulary size of 1.2 million.

their mean. This demonstrates that if the models were to be used for *scoring* text imageability, as opposed to *categorizing* text into `visual` and `non-visual` categories, CLIP and TIP-CLIP models will provide more reasonable middle-level scores for `ambiguous` text, whereas scores from BERT would either be higher or lower. We attribute this to how the underlying models are trained and how the consequent imageability scores are computed. While the BERT model is trained solely for the classification task that emphasizes discriminative encoding and the predicted probability score is used as imageability score, the distribution is bimodal. However, CLIP and TIP-CLIP are trained using image-text matching (the former, entirely; the latter, to some extent), and imageability scores are computed as the distance between the `NULL` image and input text.